Available online at

jae.cardiffuniversitypress.org

ISSN 2752-7735
The Journal of Ammonia Energy 03 (2025) 093–102

Structure and Extinction Characteristics of Methane/Ammonia/Pulverized Coal Premixed Flames

Li D[a], Yao Q[b], Li K[a], Zhang Y[a,c,*], Zhang H[a], Lyu J[a]

[a] *Key Laboratory for Thermal Science and Power Engineering of Ministry of Education, Department of Energy and Power Engineering, Tsinghua University, Beijing 100084, China*

[b] *Faculty of Metallurgical and Energy Engineering, Kunming University of Science and Technology, Kunming 650093, China*

[c] *Shanxi Research Institute for Clean Energy, Tsinghua University, Taiyuan 030032, China*

Abstract

Co-firing ammonia with pulverized coal offers a promising approach to reducing carbon emissions from coal-fired power plants. However, ammonia, as a fuel, presents challenges for combustion stability when burning compared to traditional fuels like methane. This study focuses on the extinction limits of ammonia-pulverized coal co-firing flames, a critical factor for efficient and safe combustion. A counterflow flame configuration was developed to investigate ammonia/pulverized coal premixed flames. The apparatus, with two opposed nozzles generating a planar flame, enabled the examination of gas-solid reactions. Pulverized coal was fed into the system, with methane representing the volatile matter to create a high-temperature environment for ignition. Stable methane/ammonia/pulverized coal/air premixed flames were successfully established, whose structure was observed under different conditions. The results show that in counterflow premixed flames, assisted by the methane flame, the ammonia/pulverized coal co-firing process begins with the ignition of gaseous components, forming a gaseous flame front, followed by the ignition of pulverized coal downstream in the high-temperature flue gas. The flame structure features in the coal combustion zone, the gaseous flame zone, the preheat zone, and the unburned zone. Increasing the flame stretch rate results in flame extinction, and the extinction limit of gaseous fuel plays a decisive role in the extinction of the overall gas-solid two-phase flame. For high ammonia blending ratios (50%, 75%, by energy) in the ammonia/pulverized coal mixture, the addition of pulverized coal decreases the overall extinction gaseous flame equivalence ratio at relatively high stretch rates ($\geqslant 40\ s^{-1}$) but increases the extinction gaseous flame equivalence ratio at relatively low stretch rates ($< 40\ s^{-1}$). For low ammonia blending ratios (0%, 25%), the addition of pulverized coal consistently lowers the extinction gaseous flame equivalence ratio across the range of stretch rates covered in the experiments. Additionally, the study examined synergistic effects, finding limited interaction near extinction, implying that extinction of ammonia/pulverized coal combustion closely follows the behavior of gaseous flame extinction in the mixture in weakly-stretched premixed flames. These findings provide insights for enhancing the stability of ammonia/pulverized coal co-firing.

Received: 9th Dec 24; Accepted: 31st Mar 25; Published: 11th April 25

Keywords: Co-firing ammonia with pulverized coal, Extinction limit, Counterflow flame, Combustion stability.

1. Introduction

Coal-fired power generation has long been the dominant source of global electricity production, and coal power is expected to continue playing a fundamental role as a baseload and regulatory power source in the foreseeable future [1]. However, the extensive use of coal-fired power plants has resulted in substantial emissions of carbon dioxide (CO_2), a major greenhouse gas contributing to global climate change [2]. To mitigate climate change and achieve carbon neutrality targets, there is an urgent necessity to explore clean and efficient means of carbon reduction in coal combustion.

Ammonia (NH_3), as a hydrogen energy carrier, has garnered increasing attention due to its convenient storage and transportation properties [3-5]. Ammonia can be directly utilized as a fuel to partially or completely replace fossil fuels. During combustion, ammonia does not emit CO_2 and can be synthesized through renewable energy-driven water electrolysis, achieving zero carbon emissions across its lifecycle [6]. Therefore, integrating ammonia into existing coal-fired power plants can effectively reduce CO_2 emissions while enhancing the utilization of intermittent renewable energy, which has significant practical implications.

Against this backdrop, co-firing ammonia with pulverized coal has emerged as a rising research focus. Co-firing ammonia with pulverized coal does

* Corresponding author. Tel.: +8610 6277 3153. E-mail address: yang-zhang@tsinghua.edu.cn
https://doi.org/10.18573/jae.40

not only allow for the optimal use of existing coal power infrastructure, thereby reducing retrofitting costs, but also enhances combustion efficiency through complementary fuel utilization [7, 8]. Co-firing ammonia with pulverized coal in coal-fired boilers is anticipated to be a key technology for decarbonizing power systems. However, as a gaseous fuel, ammonia exhibits combustion characteristics that significantly differ from those of solid coal, rendering the coupled combustion process complex [9, 10]. While ammonia demonstrates inferior combustion stability compared to other gaseous fuels like methane, exhibiting a flame propagation speed only about one-fifth that of methane under stoichiometric conditions and a high ignition temperature (930 K) [9], its reactivity remains significantly higher than that of pulverized coal. This relative reactivity of ammonia may influence the combustion process by altering the ignition and propagation behavior within the blended fuel system. Therefore, understanding the interaction between ammonia and pulverized coal is critical to ensuring stable and safe co-firing operations. The extinction limit is defined as the minimum concentration (equivalence ratio) at which a fuel mixture can sustain stable combustion under given conditions or, alternatively, the minimum residence time required for stable combustion at a specified equivalence ratio. Determining the extinction limit is crucial for ensuring the safe operation of combustion systems [11].

Currently, substantial research has been conducted on the fundamentals of co-firing ammonia with pulverized coal, with experimental and numerical studies predominantly focusing on drop-tube and one-dimensional furnaces (*e.g.*, [12-16]). Existing studies on the stability of co-firing ammonia with pulverized coal mainly address ignition characteristics and flame propagation speeds, whereas investigations into extinction limits remain scarce. Chen et al. [17, 18] employed a Hencken burner to investigate the ignition behavior of individual coal particles using ammonia as the carrier gas. Their results indicated that using ammonia in place of air significantly reduced the ignition delay time of pulverized coal. Co-firing ammonia with pulverized coal was found to promote the devolatilization process of coal particles and accelerate ignition. Ma et al. [19, 20] utilized an improved flat flame burner to examine the ignition and pollutant formation characteristics of co-firing ammonia with pulverized coal under controlled atmospheres. Their findings revealed a synergistic effect during co-firing, wherein increasing the ammonia blending ratio reduced the ignition delay time of coal volatiles while having minimal impact on coal particle ignition. Xia et al. [21, 22] and Hadi et al. [23] employed a spherical burner combined with OH radical imaging techniques to measure the flame propagation speed of co-firing ammonia with pulverized coal. Their results demonstrated that the flame propagation speed in co-firing exceeded that of coal particle clouds alone across all scenarios, with more pronounced effects observed for high-volatile coal. This synergistic effect was achieved under 40% O_2/60% N_2 conditions. However, whether this conclusion is applicable to conventional air or lower oxygen concentrations requires further experimental validation.

Although spherical and flat flame burners are indispensable for fundamental combustion studies, they exhibit certain limitations when investigating extinction limits. Flames in spherical burners are typically characterized by intense propagation, and their three-dimensional combustion space complicates accurate control and measurement of extinction conditions due to complex interactions between the flame and its surroundings. Flat flame burners, on the other hand, are subject to significant boundary effects and flow field distributions under near-extinction conditions, which can substantially influence the results. Consequently, measurements of extinction limits are more commonly conducted using counterflow flame burners with quasi-one-dimensional characteristics (*e.g.*, [24-26]). The residence time of the flame region in such setups can be adjusted via flame stretch rate, providing significant advantages for investigating ignition and extinction phenomena.

In summary, this study aims to investigate the extinction limits of co-firing ammonia with pulverized coal by constructing a counterflow flame test apparatus suitable for measuring these limits. The combustion characteristics and stability of co-firing ammonia with pulverized coal under varying conditions are analyzed, with the objective of identifying key factors that influence extinction limits during the co-firing process. This work seeks to provide theoretical support for the implementation of ammonia co-firing technology in practical applications such as coal-fired power plants.

2. Experimental Setup

In this study, the extinction characteristics of co-firing ammonia with pulverized coal are investigated using a counterflow single flame experimental system, as illustrated in Fig. 1. Figure 1a presents a schematic of the experimental setup, which primarily consists of five components: the gas supply system, the coal feeding system, the counterflow flame system, the cooling system, and the monitoring system. The gas supply system comprises ammonia cylinders, methane cylinders, air cylinders, and nitrogen cylinders. The flow rates of fuel, oxidizer, and shielding gas were regulated via independent pipelines and mass flow controllers. The gaseous fuel flow to the burner was regulated using mass flow controllers (Alicat Scientific MC-20SLPM, accuracy ±0.8% of reading, ±0.2% of full scale), which provided precise real-time control of flow rates with a response time of 100 ms. The coal feeding system consists of a scraper-type feeder and a drying unit, with the feeding rate controlled by adjusting the scraper speed, whose pulverized coal flow rate was calibrated at the counterflow nozzle outlet.

The counterflow flame system is composed of two symmetrically arranged nozzles, as shown in Fig. 1b. The distance (L) between the two nozzles is 2.0 cm. In practical boilers, ammonia, pulverized coal, and air are introduced into a high-temperature flue gas environment generated by combustion, where they are ignited by the high-temperature flue gases. To replicate such an environment while ensuring precise control of the flow during the experiments, methane is introduced into the premixed fuel stream, acting as the volatile matter, primarily to simulate the high-temperature flue gas environment typical in industrial boilers and to ensure stable and reliable ignition of ammonia-coal mixtures. To achieve this, the heat power provided by methane was carefully determined through preliminary experiments and thermodynamic calculations, which eventually determined that methane accounted for 60% of the thermal power, ensuring effective ignition of ammonia and pulverized coal. In the experiment, the premixed flow of methane, ammonia, pulverized coal, and air is ejected from the upper nozzle, while an inert nitrogen stream is ejected from the lower nozzle. The two streams collide between the nozzles, forming a planar stagnation surface. In addition, co-flow nitrogen is introduced to isolate the flame from external air, thereby eliminating boundary effects on the flame.

The cooling system is provided by a water chiller at the nozzle outlet to maintain consistent boundary conditions The monitoring system comprises a Raylase 30W continuous laser, a digital camera, and a high-speed camera (PCO. dimax HS4, resolution: 2000 × 2000 pixels), which are used to capture flame images under different combustion conditions, allowing for the analysis of relevant parameters of the co-firing flame structure.

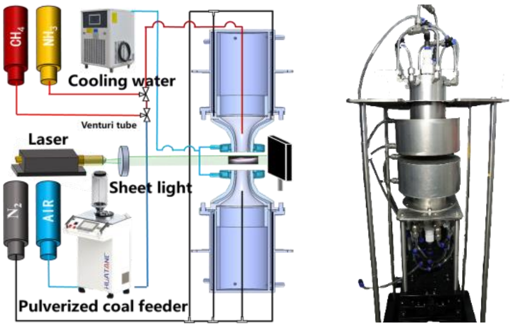

(a) (b)

Fig. 1. Experimental system and physical setup. (a) Experimental setup schematic; (b) Physical apparatus.

High-volatile bituminous coal is used in the experiments. After sieving, the particle size ranges from 75 – 96 μm. The proximate and ultimate analyses of the coal on an as-received basis are presented in Table 1. The heating value of the coal was calculated to be 22.22 MJ/kg, with a theoretical dry air requirement of 5.79 m^3/kg. The ammonia used in the experiments is industrial high-purity ammonia with a concentration exceeding 99.999% vol, and its heating value was taken as 18.6 MJ/kg.

Table. 1. Analysis of coal sample (as-received basis).

Ultimate Analysis (wt. %)				
C	H	O	N	S
59.34	3.93	15.93	1.06	0.24

Proximate Analysis (wt. %)			
Moisture	Volatile Matter	Fixed Carbon	Ash
9.5	28.8	51.7	10.0

During the experiment, the overall stretch rate (κ_{global}) of the flame can be flexibly adjusted by varying the flow velocity exiting the nozzles, and the κ_{global} value can be estimated using Eq. (1):

$$\kappa_{\text{global}} = \frac{v_{\text{U}}}{L}\left(1 + \frac{v_{\text{L}}\sqrt{\rho_{\text{L}}}}{v_{\text{U}}\sqrt{\rho_{\text{U}}}}\right) \tag{1}$$

where v_{U} and v_{L} represent the exit flow velocities (cm/s) of the upper and lower nozzles, respectively ρ_{U} and ρ_{L} denote the flow densities (g/cm^3) at the upper and lower nozzle exits; and L is the distance between the upper and lower nozzles (cm).

The overall stretch rate serves as an indicator of residence time. A higher exit velocity results in a larger stretch rate and consequently a shorter residence time. In this study, the extinction stretch rate at the brink of flame extinction (κ_{ext}) is also used to characterize the extinction limit.

The flow velocity of the gases from the upper and lower nozzles, excluding the influence of coal particles, can be calculated using Eqs. (2) and (3). In calculating the volumetric flow rate, we neglected the effect of the solid coal particles because the density of coal is more than 1000 times that of the gas. When coal contributes 40% of the total heat release, its calculated volume is much smaller than that of the gas, thereby justifying this assumption.

$$v_{\mathrm{U}} = \frac{4(V_{\mathrm{CH_4}} + V_{\mathrm{NH_3}} + V_{\mathrm{Air}})}{\pi D^2} \quad (2)$$

$$v_{\mathrm{L}} = \frac{4V_{\mathrm{N_2}}}{\pi D^2} \quad (3)$$

where the volumetric flow rates of methane, ammonia, nitrogen, and air are denoted as V_{CH4}, V_{NH3}, V_{N2}, and V_{Air}.

3. Uncertainty Analysis

κ_{global} is indirectly determined based on the flow velocities, (v_{U} and v_{L}), the distance between the nozzles (L), and the flow densities, (ρ_{U} and ρ_{L}). Therefore, the error should be determined by the uncertainties in the nozzle outlet airflow velocities (δ_{vU} and δ_{vL}) and the upper and lower nozzle spacing (δ_L). According to the theory of error propagation, the error of the flame extinction stretch rate ($\delta_{\kappa ext}$) can be expressed as Eq. (4),

$$\delta_{\kappa_{\mathrm{ext}}} = \sqrt{\left(\frac{\partial K_{\mathrm{global}}}{\partial v_{\mathrm{U}}}\delta_{v_{\mathrm{U}}}\right)^2 + \left(\frac{\partial K_{\mathrm{global}}}{\partial v_{\mathrm{L}}}\delta_{v_{\mathrm{L}}}\right)^2 + \left(\frac{\partial K_{\mathrm{global}}}{\partial \mathrm{L}}\delta_{\mathrm{L}}\right)^2} \quad (4)$$

where δ_v and δ_L represent the measurement errors of the flow velocity and the nozzle distance, respectively.

Based on Moffat's theory [27], the error in the volumetric flow rate (δ_V) can be expressed as Eq. (5),

$$\delta_V = \sqrt{(B_V)^2 + [t_{0.95}(\upsilon)\sigma_V]^2} \quad (5)$$

where B_V represents the nominal error of the calibration instrument, $t_{0.95}(\upsilon)$ corresponds to the 95% confidence interval of the t-distribution with υ degrees of freedom, and σ_V is the standard deviation obtained from the calibration curve (Eqs. (6) and (7)), *i.e.*,

$$\sigma_{V_i} = \hat{\sigma}_{V_i}\sqrt{1 + \frac{1}{n} + \frac{(V_i - \bar{V})^2}{\sum V_j^2 - (\sum V_j)^2 / n}} \quad (6)$$

where

$$\hat{\sigma}_{V_i} = \sqrt{\sum (V_j - \hat{V}_j) / (n-2)} \quad (7)$$

For the central nozzle diameter (D), vernier calipers are used during the experiment, with a resolution of 0.02 mm. Assuming a uniform distribution, the measurement errors of the central nozzle diameter and the nozzle distance, (δ_D and δ_L), are calculated as $0.02/\sqrt{3} = 0.0115$mm.

In the extinction limit measurement experiments, the equivalence ratio is indirectly determined from the flow rates of the fuel and oxidizer. Therefore, the error in the equivalence ratio (δ_Φ) is determined by the errors in the gas flow rates of the fuel and oxidizer, as well as the input error of the coal feed rate. Taking the methane/ammonia/coal experiment as an example, the equivalence ratio ϕ is defined as follows,

$$\Phi_{\mathrm{mixture}} = \frac{9.52V_{\mathrm{CH_4}} + 3.57V_{\mathrm{NH_3}} + 22.22M_{\mathrm{Coal}}}{V_{\mathrm{Air}}} \quad (8)$$

where M_{Coal} denotes the mass flow rate of coal. According to the theory of error propagation, the error in the equivalence ratio can be expressed as:

$$\delta_{\phi_{\mathrm{mixture}}} = \sqrt{\begin{aligned}&\left(\frac{\partial\phi_{\mathrm{mixture}}}{\partial V_{\mathrm{CH_4}}}\delta_{V_{\mathrm{CH_4}}}\right)^2 + \left(\frac{\partial\phi_{\mathrm{mixture}}}{\partial V_{\mathrm{NH_3}}}\delta_{V_{\mathrm{NH_3}}}\right)^2 + \\ &\left(\frac{\partial\phi_{\mathrm{mixture}}}{\partial V_{\mathrm{Air}}}\delta_{V_{\mathrm{Air}}}\right)^2 + \left(\frac{\partial\phi_{\mathrm{mixture}}}{\partial M_{\mathrm{Coal}}}\delta_{M_{\mathrm{Coal}}}\right)^2\end{aligned}} \quad (9)$$

Based on the energy ratio, the ammonia blending ratio is determined when co-firing ammonia with pulverized coal,

$$X_{\mathrm{NH_3/Coal}} = \frac{W_{\mathrm{NH_3}}}{W_{\mathrm{NH_3}} + W_{\mathrm{Coal}}} = \frac{\rho_{\mathrm{NH_3}}Q_{\mathrm{NH_3}}V_{\mathrm{NH_3}}}{\rho_{\mathrm{NH_3}}Q_{\mathrm{NH_3}}V_{\mathrm{NH_3}} + Q_{\mathrm{Coal}}M_{\mathrm{Coal}}} \quad (10)$$

where W_{NH3} and W_{Coal} denote the thermal power of ammonia and coal, respectively, while Q_{NH3} and Q_{Coal} are the heat values, ρ_{NH3} is the density of ammonia. The error in the ammonia blending ratio, according to the theory of error propagation, is expressed as follows,

$$\delta_{X_{\mathrm{NH_3/Coal}}} = \sqrt{\left(\frac{\partial X_{\mathrm{NH_3/Coal}}}{\partial V_{\mathrm{CH_4}}}\delta_{V_{\mathrm{CH_4}}}\right)^2 + \left(\frac{\partial\phi_{\mathrm{mixture}}}{\partial M_{\mathrm{Coal}}}\delta_{M_{\mathrm{Coal}}}\right)^2} \quad (11)$$

The subsequent results presented in this study are based on the experimental setup and measurement error analysis described above.

4. Results

4.1 Flame Morphology and Structure

To investigate the effects of ammonia blending on flame structure and morphology, the ammonia blending ratio, $X_{NH3/Coal}$, is defined based on the energy contribution, as shown in Eq. (10). A comparison of the counterflow flame morphology with and without pulverized coal is presented in Fig. 2. It can be observed that a large bright yellow region is visible in the flame with pulverized coal, which virtually completely obscures the gas phase flame. This bright yellow color is due to the radiation from particles during coal combustion, which to some extent hinders the observation of the flame front and the detailed structure of the co-firing flame. Thus, alternative methods are required to eliminate the effect of soot radiation.

In gas phase combustion diagnostics, specific wavelengths of chemiluminescence (e.g., OH* and CH*) are often captured to indicate the flame structure. In this study, a 430 ± 5 nm narrowband filter was installed in front of the monochrome high-speed camera to capture CH* chemiluminescence intensity, effectively removing the influence of the soot radiation layer and revealing the flame structure within the reaction zone [28, 29].

(a) (b)

Fig. 2 Comparison of counterflow flame morphology with and without pulverized coal
(a) Without pulverized coal, exposure time 1/250s;
(b) With pulverized coal, exposure time 1/1600s.

Figure 3a shows a colored photograph and a CH* image of the stable ammonia/pulverized coal flame at an ammonia blending ratio of 50%. Figure 3b shows the flame structure modeled by Xia et al. [21] during ammonia/pulverized coal combustion. A comparison reveals that both the experimental results and the model divide the flame structure into four regions along the flame propagation direction: the coal particle combustion zone, the gaseous flame zone, the preheating zone, and the unburned zone. In the coal particle combustion zone, strong orange incandescence in the color image arises from high-temperature coal particles undergoing oxidation. The gaseous flame zone is marked by bright CH* emission (visible in the CH* self-luminescence image), indicating intense gas-phase reactions of ammonia and coal volatiles. The preheating zone shows little to no visible luminosity but an elevated temperature gradient, suggesting that reactants are being heated and partially decomposed but are not yet burning vigorously. Finally, the unburned zone remains essentially dark in both the color and CH* images, with the temperature still near ambient and reactant concentrations mostly unchanged, confirming that combustion has not commenced in that region.

The observations in the present study further validate the model proposed by Xia et al. [21], with only minor discrepancies attributable to differences in flame configurations. According to Xia et al., a non-luminous reaction front characterized by radical chemiluminescence is detected upstream of the luminous flame front. In contrast, the current study demonstrates that the luminous flame front coincides with the radical chemiluminescence reaction front, suggesting that a vigorous gaseous flame front serves as the leading edge of the overall combustion process. Furthermore, as the supply of gaseous fuel is gradually reduced, the solid combustion flame extinguishes following the extinction of the gaseous flame. Based on the results of the experiments, it is reasonable to infer that after the ignition of gaseous species in the preheating zone, the temperature increases, leading to the pyrolysis of solid coal particles and the release of volatiles, which further enhance the combustion of the gas-phase flame.

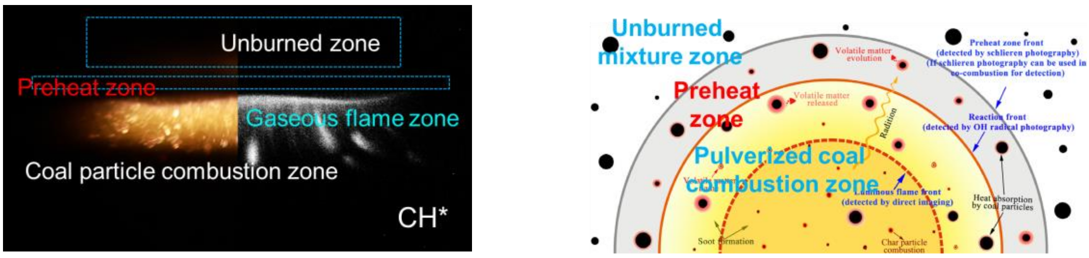

(a) (b)

Fig. 3 Ammonia/pulverized coal co-firing flame structure under stable combustion conditions. (a) Experimental result (b) Proposed by Xia et al. [21]

Therefore, the present experiment confirmed that the gas phase flame dominated the flame structure of co-firing ammonia with pulverized coal.

Figure 4 illustrates the effect of increasing the ammonia blending ratio on the flame morphology. Figures 4a and 4b respectively present the CH* chemiluminescence images of the flame captured using a 430 nm narrowband filter and the corresponding color flame images taken with a digital camera. In the presence of a constant equivalence ratio of 1, increasing the ammonia blending ratio produces an increase in the thickness of the luminous flame front, indicating that the addition of ammonia promotes the combustion of the pulverized coal flow, as many researchers have found. (*e.g.* [19, 31]).

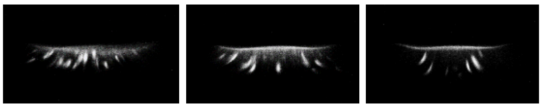

(a) CH* chemiluminescence image of flame with pulverized coal (Exposure time: 20 ms)*

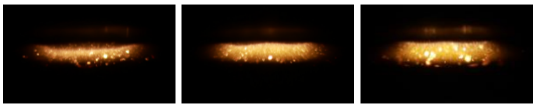

(b) Color image of flame with pulverized coal (Exposure time: 0.625 ms)

$X_{NH3/Coal}$=25% $X_{NH3/Coal}$=50% $X_{NH3/Coal}$=75%

Fig. 4 The Effect of increasing ammonia blending ratio on flame morphology ($\Phi_{mixture}$ = 1, W_{total} = 0.18 W, κ_{global} = 27 – 29 s). Fig. 4a was taken with a 430 nm narrowband filter, exposure time 20 ms; Fig. 4b was taken with an exposure time of 0.625 ms.

It can also be observed from Fig. 4 that during co-firing ammonia with pulverized coal, coal particle ignition occurs exclusively downstream of the gas phase flame front in the high-temperature zone. The flame intensity is significantly stronger with the addition of pulverized coal, indicating that the co-firing process involves gas phase ignition followed by pyrolysis of solid coal particles due to heating by the flame front and surrounding high-temperature flue gas. The released volatiles, in turn, promote the combustion of the gas phase flame. Due to the high Stokes number of coal particles (rough estimations indicate that the Stokes number falls approximately within the range of 26 to 43), they can pass through the flame front during movement and reach the vicinity of the stagnation plane, where they undergo ignition when the temperature is sufficiently high due to convective and radiative heat transfer.

Further, it was found that after removing the influence of the particle radiation layer, the CH* intensity of the flame initially increased and then decreased with increasing ammonia blending ratio (Fig. 4a). This probably indicates a synergistic effect of ammonia addition on flame intensity, which warrants further investigation.

4.2 Extinction Characteristics

In this study, the extinction limit of the counterflow flame was measured based on the steady-state method, employing a single flame structure. As compared to a dual-flame symmetrical configuration, the single flame structure experiences greater heat loss to both ends, facilitating identification of the flame's critical extinction state. Due to the gas-solid mixing involved and the necessity of methane to provide a high-temperature flue gas environment, all experimental conditions were set by varying the ammonia and coal ratios while maintaining a fixed thermal contribution from methane. The equivalence ratio of each mixture, $\Phi_{mixture}$, was defined as shown previously in Eq. (8).

The method for determining the extinction stretch rate for each set of conditions was as follows: First, a condition with a relatively low stretch rate was established initially, and a stable counterflow flame was formed. Air flow rate was then gradually increased, causing the flame to be weakened and approach the extinction limit. When the flame reached a critical state, where it was about to extinguish but had not yet extinguished, each increment in the air flow rate was limited to no more than 1.5%. This process was repeated until the flame extinguished, and the overall stretch rate of the final condition κ_{global} was taken as the extinction stretch rate κ_{ext} at that corresponding equivalence ratio. Subsequently, the fuel flow rate was increased while keeping the ammonia and coal blending ratio constant, and the above process was repeated to determine the equivalence ratio and corresponding extinction stretch rate for that ammonia blending ratio. The flowchart of the flame extinction process is shown in Fig. 5. Initially, the luminous flame was relatively thick and bright, but as the air flow increased, the equivalence ratio decreased and the flame propagation speed reduced. The flame front moved towards the stagnation plane, and as the available reaction residence time decreased, the flame’s brightness gradually diminished until it coincided with the stagnation plane and extinguished.

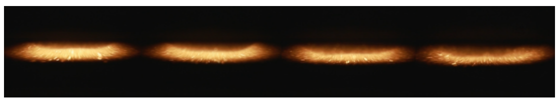

Fig. 5 Process of flame extinction ($\Phi_{mixture}$ = 1, W_{total} = 0.18 W).

Figure 6 presents the variation of the κ_{ext} value with the equivalence ratio $\Phi_{mixture}$ for different ammonia blending ratios. Similar to pure gaseous flames, the κ_{ext} value of the ammonia/pulverized coal flame increases approximately with the equivalence ratio. It can also be observed that for $\Phi_{mixture} < 1.1$, the κ_{ext} value increases with increasing ammonia blending ratio. Increasing the ammonia blending ratio results in a more stable temperature field in the gaseous flame front, and the combustion reaction is more complete, which further enhances flame stability, resulting in flame extinction occurring at higher stretch rates. Additionally, an interesting observation is that within the equivalence ratio range of 1.05 – 1.10, ammonia blending ratios of 75%, 50%, and 25% yield comparable extinction stretch rates. This phenomenon warrants further investigation in future studies.

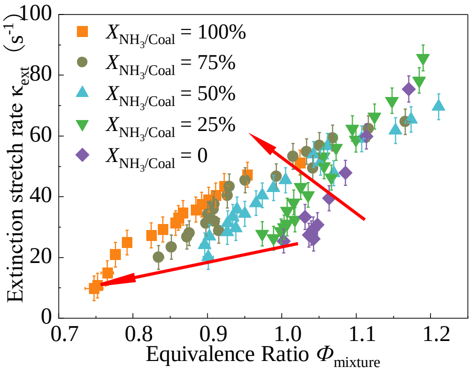

Fig. 6. Extinction stretch rate variation with equivalence ratio at different ammonia blending ratios

As it is found in Figs. 3 and 4 that the gaseous flame leads the stable flame front, to further investigate the effect of gaseous flame on the extinction characteristics of the ammonia/pulverized coal co-firing, a special equivalence ratio, $\Phi_{NH3/CH4}$, was defined to include only the gaseous phase of ammonia and methane, as expressed in Eq. (12),

$$\Phi_{NH_3/CH_4} = \frac{9.52V_{CH_4} + 3.57V_{NH_3}}{V_{Air}} \qquad (12)$$

The difference in extinction equivalence ratio was compared between mixtures with and without pulverized coal addition is presented in Fig. 7. Two key observations were identified. First, although there are certain disparities between the extinction limit curves for the two conditions with and without pulverized coal, the extinction curves are rather close, indicating that the stability of the gas phase flame plays a decisive role in maintaining overall ammonia/pulverized coal co-firing flame stability under the near-extinction conditions. Second, it can be observed that for ammonia blending ratios greater than 50% (Figs. 7a and 7b), a critical overall stretch rate ($\kappa_{critical} \approx 40$ s^{-1}) can be identified. When $\kappa > \kappa_{critical}$, the addition of pulverized coal increases the extinction equivalence ratio, indicating that the flame becomes less stable with the pulverized coal addition. Conversely, when $\kappa < \kappa_{critical}$, the addition of pulverized coal slightly reduces the extinction equivalence ratio, thereby enhancing the stability of the mixed flame. This effect becomes more pronounced at higher ammonia blending ratios (50%, 75%). For lower ammonia blending ratios (0%, 25%), as shown in Figs. 7c and 7d, adding pulverized coal consistently reduces the extinction equivalence ratio, making the flame more stable.

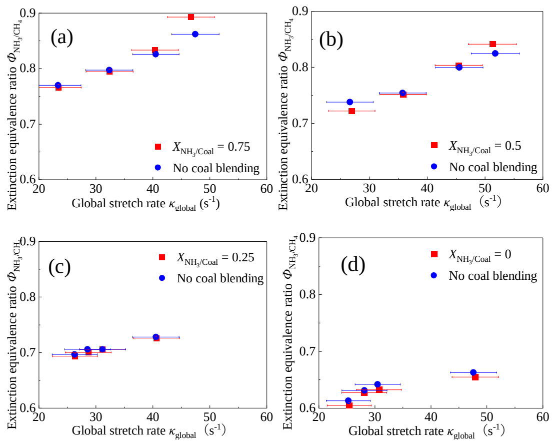

Fig. 7. Extinction gaseous fuel equivalence ratio variation with global stretch rate at different ammonia blending ratios; a) 75%; b) 50%; c) 25%; d) 0%.

4.3 Discussion on the Synergistic Effect

Finally, the synergistic effect of co-firing ammonia with pulverized coal was explored. We choose 3 points in Fig. 4, points with $\Phi_{mixture}$ = 0.9, 1.0, and 1.1 are selected, and the κ_{ext} value as a function of ammonia blending ratio is plotted for these equivalence ratios, as shown in Fig. 8. It can be seen that as the ammonia blending ratio increases, the extinction stretch rate generally increases monotonically, with no significant synergistic effect observed. This is because, during near-extinction conditions, the extinction limit of the gaseous fuel plays a decisive role in the extinction of the entire flame. During the combustion process of the ammonia-coal flame, the gas phase ammonia is ignited first, providing a continuous heat source that subsequently ignites the solid coal particles. During the extinction process, the gaseous flame also extinguishes first, making it difficult for the coal particle combustion to be sustained, leading to synchronized extinction. For the near-limit flames with limited residence time, the combustion of pulverized coal is relatively weak and is strongly dependent on the behavior of the gaseous flame, making this outcome predictable. As shown in Fig. 9, analyzing only the extinction equivalence ratio of the gaseous flame reveals that the gaseous flames are indeed ultra-lean near-limit flames in the present study. The extinction equivalence ratio changes monotonically with the ammonia blending ratio, and thus no clear synergistic effect between ammonia and pulverized coal combustion is observed in the overall flame. These findings sightly differ from those in Ref. [19, 21, 30].

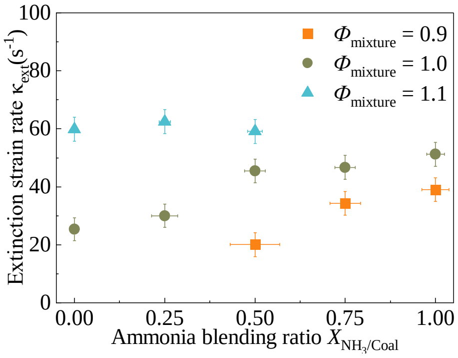

Fig. 8 Variation of extinction stretch rate with ammonia blending ratio at different mixture equivalence ratios

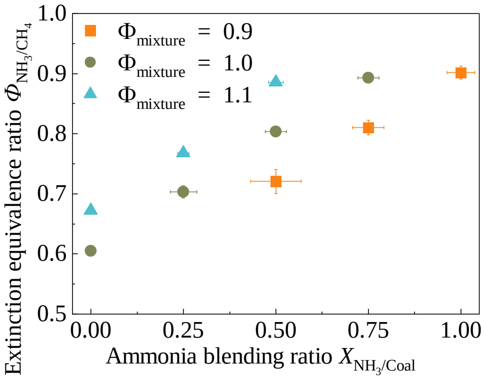

Fig. 9 Variation of extinction gaseous fuel equivalence ratio with ammonia blending ratio at different mixture equivalence ratios

It is also noteworthy that when $\Phi_{mixture}$ = 1.1, the κ_{ext} value begins to decrease with increasing ammonia blending ratio, as observed in Fig. 6. At this point, the fuel is relatively rich, and the oxygen concentration is lower. Further research should be conducted on this equivalence ratio and subsequent conditions to explore the synergistic effects of ammonia and coal during near-extinction conditions.

5. Conclusions

We develop a counterflow flame experimental setup to measure the extinction limits. The combustion characteristics and extinction limits of co-firing ammonia with pulverized coal under various conditions were examined, leading to the following conclusions:

a) The specific structure of the ammonia/pulverized coal counterflow flame was determined. The flame structure is featured by the unburned zone, preheating zone, gaseous flame zone, and coal combustion zone. The ignition of gaseous flames occurs first, followed by the pyrolysis of coal particles, which produces volatiles which enhance gas phase combustion. The ammonia addition promotes the combustion of pulverized coal as indicated by the thickened thickness of the luminous flame front.

b) The extinction stretch rate of the flame was measured for different ammonia blending ratios as a function of the mixture equivalence ratio. The stability of the gaseous flame front plays a decisive role in the extinction of the entire ammonia/pulverized coal co-firing flames. For high ammonia blending ratios (50%, 75%, by energy) in the ammonia/pulverized coal mixture, the addition of pulverized coal decreases the overall extinction gaseous flame equivalence ratio at relatively high stretch rates (⩾ 40 s-1) but increases the extinction gaseous flame equivalence ratio at relatively low stretch rates (< 40 s-1). For low ammonia blending ratios (0%, 25%), the addition of pulverized coal consistently lowers the extinction gaseous flame equivalence ratio across the range of stretch rates covered in the experiments.

c) Within the range of mixture equivalence ratios less than 1.1, no synergistic effect was observed in the extinction fuel lean side with varying ammonia blending ratios. For the near-limit flames with limited residence time, the combustion of pulverized coal is relatively weak and is strongly dependent on the behavior of the gaseous flame, resulting in no apparent synergistic effect between ammonia and pulverized coal combustion.

Acknowledgments

This research was jointly supported by the National Natural Science Foundation of China (Grant No. U24B2069) and the 'Champion Project' of Shanxi Institute of Clean Energy Research, Tsinghua University (Grant No. 2023JZ0501001).

Conflicts of Interest

The authors declare no conflict of interest. The funders had no role in the design of the study; in the collection, analyses, or interpretation of data; in the writing of the manuscript, or in the decision to publish the results.

References

[1] Steckel JC, Edenhofer O, Jakob M. Drivers for the renaissance of coal, Proc Nat Academy Sci 2015 112: E3775-E3781. https://doi.org/10.1073/pnas.1422722112

[2] Munawer ME. Human health and environmental impacts of coal combustion and post-combustion wastes, J Sust Mining 2018 17: 87-96. https://doi.org/10.1016/j.jsm.2017.12.007

[3] Kobayashi H, Hayakawa A, Somarathne KDKA, Okafor EC. Science and technology of ammonia combustion, Proc Combust Inst 2019 37: 109-133. https://doi.org/10.1016/j.proci.2018.09.029

[4] Elbaz AM, Wang S, Guiberti TF, Roberts WL. Review on the recent advances on ammonia combustion from the fundamentals to the applications, Fuel Comms 2022 10: 100053 https://doi.org/10.1016/j.jfueco.2022.100053

[5] Wang Q, Hu Z, Shao W, Wang Z, Liu H, Li X, Cui D. The present situation, challenges, and prospects of the application of ammonia–coal co-firing technology in power plant boilers, J Energy Inst 2024 113: 101531. https://doi.org/10.1016/j.joei.2024.101531

[6] Genichiro N. Development of Co-Firing Method of Pulverized Coal and Ammonia to Reduce Greenhouse Gas Emissions. IHI Engin Review 2020 53(1): 1-10.

[7] Zhang J, Ito T, Ishii H, Ishihara S, Fujimori T. Numerical investigation on ammonia co-firing in a pulverized coal combustion facility: Effect of ammonia co-firing ratio, Fuel 2020 267: 117166. https://doi.org/10.1016/j.fuel.2020.117166

[8] Yamamoto A, Kimoto M, Ozawa Y, Hará S. Basic co-firing characteristics of ammonia with pulverized coal in a single burner test furnace. 2018 AIChE Annual Meeting; 2018, AIChE.

[9] Valera-Medina A, Xiao H, Owen-Jones M, David WIF, Bowen PJ. Ammonia for power, Prog Energy Combust Sci 2018 69: 63-102. https://doi.org/https://doi.org/10.1016/j.pecs.2018.07.001

[10] Miura K. Mild conversion of coal for producing valuable chemicals, Fuel Proces Tech 2000 62: 119-135. https://doi.org/https://doi.org/10.1016/S0378-3820(99)00123-X

[11] Ichimura R, Hadi K, Hashimoto N, Hayakawa A, Kobayashi H, Fujita O. Extinction limits of an ammonia/air flame propagating in a turbulent field, Fuel 2019 246: 178-186. https://doi.org/10.1016/j.fuel.2019.02.110

[12] Wang X, Fan W, Chen J, Zhang H. Experimental study and kinetic analysis of NO emission characteristics in ammonia/coal co-firing process with different ammonia injection methods, J Energy Inst 2024 114: 101609. https://doi.org/10.1016/j.joei.2024.101609

[13] Hu S, Zhang Y, Ni Y, Yu X, Rong Y, Cen K, Zhou H. Experimental investigation of combustion and ash deposition characteristics of coal-NH3 cofiring in a 200 kW furnace, Fuel 2023 350: 128797. https://doi.org/10.1016/j.fuel.2023.128797

[14] Tan J, He Y, Zhu R, Zhu Y, Wang Z. Experimental study on co-firing characteristics of ammonia with pulverized coal in a staged combustion drop tube furnace, Proc Combust Inst 2023 39: 3217-3225. https://doi.org/10.1016/j.proci.2022.07.032

[15] Wang Z, Jia Z, Zhao C, Xiao Y, Feng S, Chu H. Effect of ammonia on the characteristics of coal combustion, J Energy Inst 2023 109: 101275. https://doi.org/10.1016/j.joei.2023.101275

[16] Chen P, Jiang B, Wang H, Gu M, Fang Y, Wang P. Experimental and theoretical calculations study on heterogeneous reduction of NO by char/NH3 in the reduction zone of ammonia co-firing with pulverized coal: Influence of mineral Fe, Fuel 2022 310: 122374. https://doi.org/10.1016/j.fuel.2021.122374

[17] Chen C, Wang Z, Zhu R, Tan J, He Y, Cen K. Co-firing characteristics and fuel-N transformation of ammonia/pulverized coal binary fuel, Fuel 2023 337: 126857. https://doi.org/10.1016/j.fuel.2022.126857.

[18] Chen C, Wang Z, He Y, Weng W, Cen K. Ignition characteristics of single coal particles under ammonia co-firing conditions, Combust Flame 2024 263: 113385. https://doi.org/10.1016/j.combustflame.2024.113385.

[19] Ma P, Huang Q, Wu Z, Lyu J, Li S. Optical diagnostics on coal ignition and gas phase combustion in co-firing ammonia with pulverized coal on a two-stage flat flame burner, Proc Combust Inst 2023 39: 3457-3466. https://doi.org/10.1016/j.proci.2022.07.221.

[20] Ma P, Nicolai H, Huang Q, Debiagi P, Berkel LL, Stagni A, Yang Y, Hasse C, Li S. Numerical investigation on pyrolysis and ignition of ammonia/coal blends during co-firing, Combust Flame 2024 261: 113268. https://doi.org/10.1016/j.combustflame.2023.113268.

[21] Xia Y, Hadi K, Hashimoto G, Hashimoto N, Fujita O. Effect of ammonia/oxygen/nitrogen equivalence ratio on spherical turbulent flame propagation of pulverized coal/ammonia co-combustion, Proc Combust Inst 2021 38: 4043-4052. https://doi.org/10.1016/j.proci.2020.06.102

[22] Xia Y, Hashimoto N, Fujita O. Turbulent flame propagation mechanism of polymethylmethacrylate particle cloud–ammonia co-combustion, Combust Flame 2022 241: 112077.

https://doi.org/10.1016/j.combustflame.2022.112077
[23] Hadi K, Ichimura R, Hashimoto G, Xia Y, Hashimoto N, Fujita O. Effect of fuel ratio of coal on the turbulent flame speed of ammonia/coal particle cloud co-combustion at atmospheric pressure, Proc Combust Inst 2021 38: 4131-4139. https://doi.org/10.1016/j.proci.2020.06.358
[24] Ji C, Dames E, Wang H, Egolfopoulos FN. Propagation and extinction of benzene and alkylated benzene flames, Combust Flame 2012 159: 1070-1081. https://doi.org/10.1016/j.combustflame.2011.10.017.
[25] Li B, Liu N, Zhao R, Zhang H, Egolfopoulos FN. Flame propagation of mixtures of air with high molecular weight neat hydrocarbons and practical jet and diesel fuels, Proc Combust Inst 2013 34: 727-733. https://doi.org/10.1016/j.proci.2012.05.063
[26] Cooke JA, Bellucci M, Smooke MD, Gomez A, Violi A, Faravelli T, Ranzi E. Computational and experimental study of JP-8, a surrogate, and its components in counterflow diffusion flames, Proc Combust Inst 2005 30: 439-446. https://doi.org/10.1016/j.proci.2004.08.046
[27] Moffat RJ. Describing the uncertainties in experimental results, Exp Thermal Fluid Sc 1988 1: 3-17. https://doi.org/10.1016/0894-1777(88)90043-X.
[28] De Leo M, Saveliev A, Kennedy LA, Zelepouga SA. OH and CH luminescence in opposed flow methane oxy-flames, Combust Flame 2007 149: 435-447. https://doi.org/10.1016/j.combustflame.2007.01.008
[29] Zhang T, Guo Q, Liang Q, Dai Z, Yu G. Distribution characteristics of OH*, CH*, and C2* luminescence in CH4/O2 co-flow diffusion flames, Energy Fuels 2012 26: 5503-5508. https://doi.org/10.1021/ef300970a
[30] Taniguchi M. Flame Propagation Velocity for Co-combustion of Pulverized Coals and Gas Fuels, Energy Fuels 2021 35: 6305-6314. https://doi.org/10.1021/acs.energyfuels.1c00014
[31] Meller D, Engelmann L, Wollny P, et al. Evaluation of ammonia co-firing in the CRIEPI coal jet flame using a three mixture fraction FPV-LES[J]. Proc Combust Inst 2023 39(3): 3615-3624. https://doi.org/10.1016/j.proci.2022.07.182